First-order reliability method-based system reliability analyses of corroding pipelines considering multiple defects and failure modes

Article *in* Structure and Infrastructure Engineering · February 2017

DOI: 10.1080/15732479.2017.1285330

2 authors:

Changqing Gong
The University of Western Ontario

Wenxing Zhou
The University of Western Ontario

Taylor & Francis
Taylor & Francis Group

Structure and Infrastructure Engineering

Maintenance, Management, Life-Cycle Design and Performance

ISSN: 1573-2479 (Print) 1744-8980 (Online) Journal homepage: http://www.tandfonline.com/loi/nsie20

First-order reliability method-based system reliability analyses of corroding pipelines considering multiple defects and failure modes

Changqing Gong & Wenxing Zhou

To cite this article: Changqing Gong & Wenxing Zhou (2017): First-order reliability method-based system reliability analyses of corroding pipelines considering multiple defects and failure modes, Structure and Infrastructure Engineering, DOI: 10.1080/15732479.2017.1285330

To link to this article: http://dx.doi.org/10.1080/15732479.2017.1285330

Published online: 07 Feb 2017.

STRUCTURE AND INFRASTRUCTURE ENGINEERING, 2017
http://dx.doi.org/10.1080/15732479.2017.1285330

Taylor & Francis
Taylor & Francis Group

First-order reliability method-based system reliability analyses of corroding pipelines considering multiple defects and failure modes

Changqing Gong and Wenxing Zhou

Department of Civil and Environmental Engineering, The University of Western Ontario, London, Canada

ABSTRACT
A methodology that employs the first-order reliability method is proposed to evaluate the time-dependent system reliability of a segment of a pressurised steel pipeline containing multiple active corrosion defects. The methodology considers the leak and burst failure modes of the pipe segment and takes into account the correlations among limit state functions at different corrosion defects. The methodology involves first constructing two linearised equivalent limit state functions for the pipe segment in the standard normal space and then evaluating the probabilities of leak and burst of the segment incrementally over time based on the equivalent limit state functions. The applicability and accuracy of the proposed methodology is illustrated through system reliability analyses of three pipeline examples, each containing ten active corrosion defects whose growth over time is characterised by the linear, nonlinear and homogeneous gamma process-based models.

ARTICLE HISTORY
Received 8 June 2016
Revised 11 November 2016
Accepted 15 November 2016

KEYWORDS
Corrosion; first-order reliability method; failure mode; pipelines; system reliability; equivalent limit state function

1. Introduction

Metal-loss corrosion is one of the leading causes for failures of pressurised steel oil and gas pipelines (Nessim, Zhou, Zhou, & Rothwell, 2009). The reliability-based corrosion management program is being increasingly adopted by pipeline operators (Kariyawasam, & Peterson, 2010; Huyse, & Brown, 2012) because it can effectively deal with the various uncertainties that are either inherent to the corrosion process or involved in the inspection and assessment of corrosion defects. Inline inspection (ILI) tools, which are generally based on the magnetic flux leakage (MFL) or ultrasonic (UT) technology, are now being routinely used by pipeline operators to detect, locate and size corrosion defects on pipelines with the inspection interval varying from a few to ten years (Kariyawasam, & Peterson, 2010). A key component of the reliability-based integrity management of a corroding pipeline is to evaluate its time-dependent failure probabilities, based on the defect information reported by the ILI tool, such that effective inspection and maintenance strategies can be developed to ensure the safety and economic viability of the pipeline.

Metal-loss corrosion defects can exist on both the external and internal surfaces of a pipeline. A typical defect is three-dimensional (i.e. volumetric) and characterised by its length (in the pipeline longitudinal direction), width (in the circumferential direction) and maximum depth (in the through-pipe wall thickness direction). Figure 1 schematically illustrates the geometry of a representative defect. The defect grows in size over time and can cause the pipeline to fail by one of two failure modes, namely leak and burst (Zhou, 2010). A leak occurs if the defect penetrates the pipe wall, whereas a burst occurs if the remaining ligament of the pipe wall at the defect undergoes plastic collapse due to the internal pressure before the defect penetrating the pipe wall.

It should be noted that the potential scenario of the failure model escalation, i.e. a leak escalating to a burst due to, for example, the development of a crack after the defect penetrates the pipe wall, is not considered in this study. Given that the consequences in terms of human safety, environmental impact and property damage associated with leaks and bursts of pipelines can be markedly different (Nessim, Zhou, Zhou, & Rothwell, 2009). Separating these two failure modes in the reliability analysis has important implications for the risk assessment of corroding pipelines and prioritisation of corrosion mitigation measures. Because a failed pipe segment, by leak or burst, is typically dealt with (e.g. repaired or taken out of service) within a short time frame such as several days, the occurrence of one failure mode essentially eliminates the potential occurrence of the other failure mode. Therefore, leak and burst should be considered as two competing failure modes in the reliability analysis.

A pipeline segment, such as a pipe joint with a typical length of 10–20 m long (Al-Amin, & Zhou, 2014), may contain multiple active corrosion defects. Since failure at any of the defects implies failure of the pipeline segment, the reliability of the segment should be evaluated as the reliability of a series system. Note that failures at different defects are in general statistically correlated, for example, due to the correlation between the defect sizes and pipe properties (e.g. pip wall thickness and yield strength) at

CONTACT Wenxing Zhou wzhou@eng.uwo.ca

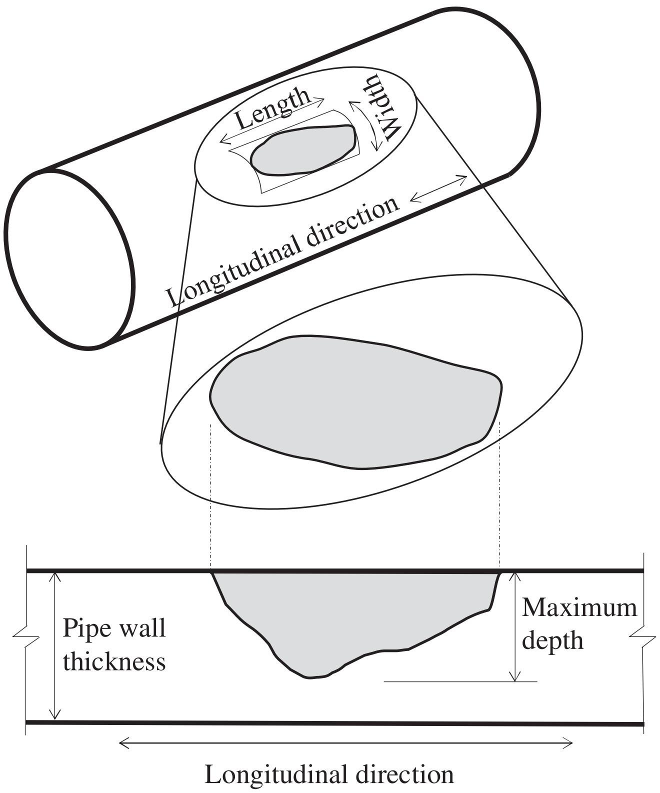

Figure 1. Schematic illustration of the geometry of a typical corrosion defect.

different defects. Such correlations must be considered in the evaluation of the system reliability of the pipeline segment.

The simple Monte Carlo simulation (MCS) can be straightforwardly applied to evaluate the probabilities of leak and burst of the segment (Zhou, 2010); however, this approach is computationally costly considering that the probability of failure of a given segment can be quite low (e.g. $<10^{-6}$) and that many segments may need to be analysed for a given pipeline system. An enhanced MCS technique has been employed to calculate failure probabilities of pipe segments containing multiple corrosion defects in a recent study (Leira, Næss, & Næss, 2016); however, only the burst failure mode was considered in the study.

The efficient first-order reliability method (FORM) (Melchers, 1999; Der Kiureghian, 2005; Low, & Tang, 2007) is widely used to evaluate the reliability of engineering systems. The application of FORM to evaluate the failure probabilities of pipelines with corrosion defects has been reported in the literature (Teixeira, Soares, Netto, & Estefen, 2008; Sahraoui, Khelif, & Chateauneuf, 2013; Zhang, & Zhou, 2014; Miran, Huang, & Castaneda, 2016). Teixeira et al. (2008) and Sahraoui et al. (2013) employed the FORM to evaluate the probability of burst of a pipeline at a given corrosion defect, but did not consider the leak failure mode in the analysis. Zhang and Zhou (2014) developed a FORM-based methodology to evaluate the time-dependent probabilities of leak and burst at a single active corrosion defect on a pipeline. However, the methodology is not applicable to evaluating the time-dependent probabilities of leak and burst of a pipe segment containing multiple active corrosion defects. Miran et al. (2016) evaluated the system failure probability of pipe segments considering multiple defects and multiple failure modes (i.e. small leak, large leak and rupture) using the FORM. However, their study did not consider the potential correlations among failures at different defects.

The objective of the work reported in this article is to develop an efficient FORM-based methodology to evaluate the time-dependent probabilities of leak and burst of a pipeline segment containing multiple active corrosion defects by taking into account the correlations among failures at different defects. The methodology includes two key components. First, two equivalent linearised time-dependent limit state functions, one for leak and the other for burst, are constructed in the standard normal space for the multiple defects on the pipeline segment, based on the FORM results obtained for individual failure modes associated with individual defects. Second, formulations are developed for computing the incremental probabilities of leak and burst of the pipeline segment over a short time increment based on the equivalent limit state functions. The proposed methodology is illustrated using three numerical examples, in which different models characterising the growth of corrosion defects are employed. The accuracy of the proposed methodology is demonstrated by comparing the evaluated probabilities of leak and burst with the corresponding values obtained from the simple MCS analysis.

2. Limit state functions

Consider a pipeline segment with a total of n active corrosion defects. The limit state function, $g_i^s(t)$, for the ith defect (i = 1, 2, …, n) penetrating the pipe wall at a given time t is given by:

$$g_i^s(t) = \varphi wt_i - d_i(t) \tag{1}$$

where wt_i is the pipe wall thickness at the location of the ith defect; $d_i(t)$ is the maximum defect depth (see Figure 1) at time t, and φ ($\varphi \le 1$) is a reduction factor to account for the fact that the remaining ligament of the pipe wall is prone to developing cracks that could lead to a leak once the defect is sufficiently deep (Al-Amin, & Zhou, 2014). A typical value of φ is 0.8 (Caleyo, Gonzalez, & Hallen, 2002; Zhou, 2010). Note that both random variable- and stochastic process-based models have been reported in the literature to characterise the defect growth (Zhou, 2010; Lu, Xie, & Pandey, 2013; Gomes, & Beck, 2014).

The limit state function, $g_i^c(t)$, for plastic collapse of the remaining ligament at the ith defect at time t is given by:

$$g_i^c(t) = p_{ci}(t) - p_i \tag{2}$$

where $p_{ci}(t)$ is the burst pressure capacity of the pipeline segment at the ith defect at time t and p_i is the internal pressure at the ith defect. Although the pipe internal pressure is controlled during operation, there are inevitable random pressure fluctuations over time. Therefore, the internal pressure should ideally be modeled as a time-dependent random process. However, such a model will significantly complicate the proposed methodology. Given that the uncertainty in the internal pressure is in general much less than that in the corrosion growth process (Canadian Standards Association (CSA), 2015), the internal pressure is characterised by a time-independent random variable instead of a time-dependent random process in this study.

Empirical and semi-empirical models for evaluating p_{ci} are well reported in the literature (Zhou, & Huang, 2012). Although in various forms, these models are in general functions of the depth and length (i.e. in the longitudinal direction of the pipeline) of the corrosion defect, pipe geometry (i.e. diameter and wall thickness) and material strength (e.g. yield strength or tensile strength). For example, p_{ci} can be evaluated using the well-known ASME B31G Modified model (Kiefner, & Vieth, 1989) as follows:

$$p_{ci} = \xi_i \frac{2wt_i(\sigma_{yi} + 68.95)}{D_i}\left[\frac{1 - \frac{0.85d_i}{wt_i}}{1 - \frac{0.85d_i}{M_i wt_i}}\right], \quad \frac{d_i}{wt_i} \le 0.8 \tag{3}$$

$$M_i = \begin{cases} \sqrt{1 + 0.6275\frac{l_i^2}{D_i wt_i} - 0.003375\frac{l_i^4}{(D_i wt_i)^2}}, & \frac{l_i^2}{D_i wt_i} \le 50 \\ 3.3 + 0.032\frac{l_i^2}{D_i wt_i}, & \frac{l_i^2}{D_i wt_i} > 50 \end{cases} \tag{4}$$

where ξ is the model error associated with the B31G Modified model (Zhou, & Huang, 2012); D is the pipe outside diameter; σ_y and σ_y + 68.95 (MPa) are the yield strength and empirically defined flow stress of the pipe steel, respectively; M is the so-called Folias factor; l is the defect length, and the subscript i denotes the value of the variable corresponding to the ith defect. For simplicity, the dependence of d_i and l_i on time is made implicit in Equations (3) and (4).

Let $P_l(t)$ and $P_b(t)$ denote the cumulative probabilities of leak and burst of the pipeline segment, respectively, within a time interval $[0, t]$. Further let t_i^s denote the time at which the ith defect just penetrates the pipe wall, and t_i^c denote the time at which plastic collapse takes place at the ith defect due to the internal pressure. Because of the competing nature of the leak and burst failure modes, $P_l(t)$ and $P_b(t)$ are defined as follows using t_i^s and t_i^c:

$$P_l(t) = \text{Prob}\left[\left(0 \le \min_i \left\{t_i^s\right\} \le t\right) \cap \left(\min_i \left\{t_i^s\right\} < \min_i \left\{t_i^c\right\}\right)\right] \tag{5a}$$

$$P_b(t) = \text{Prob}\left[\left(0 \le \min_i \left\{t_i^c\right\} \le t\right) \cap \left(\min_i \left\{t_i^c\right\} < \min_i \left\{t_i^s\right\}\right)\right] \tag{5b}$$

where ∩ denotes the intersection of two events.

3. FORM-based time-dependent system reliability analysis of corroding pipelines

3.1. Overview of FORM

FORM analysis with respect to a single limit state function involves transforming the random variables included in the limit state function into the standard normal space and then evaluating the reliability index β, which equals the minimum distance from the origin to the limit state surface in the standard normal space (Der Kiureghian, 2005). The failure probability is then approximated by $\Phi(-\beta)$, where $\Phi(\bullet)$ is the standard normal cumulative distribution function (CDF). This approximation is equivalent to that the limit state function in the standard normal space is replaced by a linearised limit state function (or safety margin) and that the limit state surface is replaced by a hyperplane that is tangential to the limit state surface at the design point (Der Kiureghian, 2005). The unit vector that is normal to the limit state surface at the design point and points toward the failure domain is a measure of the sensitivity of the reliability index to the standard normal variates transformed from the random variables in the original space. A summary of the formulations involved in the FORM is presented in Appendix A for interested readers.

For a series system with n limit state functions that are statistically dependent, the failure probability of the system, P_f, can be evaluated as (Der Kiureghian, 2005):

$$P_f = 1 - \Phi_n(\boldsymbol{\beta}, \boldsymbol{R}) \tag{6}$$

where $\boldsymbol{\beta} = [\beta_1, \beta_2, \ldots, \beta_n]^{\mathrm{T}}$ is the vector of reliability indices corresponding to the n limit state functions; the superscript T denotes transposition; $\boldsymbol{R} = \{r_{ij}\}$ $(i, j = 1, 2, \ldots, n)$ is the matrix of the correlation coefficients between linearised safety margins associated with limit state functions i and j in the standard normal space, and $\Phi_n(\bullet, \bullet)$ is the n-dimensional standard normal cumulative distribution function. The correlation coefficient $r_{ij} = \boldsymbol{\alpha}_i^T \boldsymbol{\alpha}_j$, where $\boldsymbol{\alpha}_i$ and $\boldsymbol{\alpha}_j$ are the unit normal vectors (pointing toward the failure domain) to the limit state functions i and j, respectively, at their corresponding design points in the standard normal space (Der Kiureghian, 2005). Note that the dimension of $\boldsymbol{\alpha}_i$ $(j = 1, 2, \ldots, n)$ is the same as the dimension of the vector of random variables involved in the system. In this study, the Genz's method (Genz, 1992) as implemented in the Matlab® function QSIMVNV (http://www.math.wsu.edu/faculty/genz/software/software.html) is employed to evaluate $\Phi_n(\boldsymbol{\beta}, \boldsymbol{R})$.

3.2. Equivalent limit state functions for corroding pipelines

The pipeline segment containing n active corrosion defects described in Section 2 can be considered to include two series systems, one system with n limit state functions ($g_i^s(t)$, $i = 1, 2, \ldots, n$) representing the defect penetrating the pipe wall and the other system with n limit state functions ($g_i^c(t)$) representing the plastic collapse. Let the union of all the random variables (e.g. pipe wall thicknesses, yield strengths, internal pressures and defect sizes) involved in $g_i^s(t)$ and $g_i^c(t)$ $(i = 1, 2, \ldots, n)$ be represented by an m-dimensional vector $\boldsymbol{X}$. The probabilistic characteristics of some of the random variables included in $\boldsymbol{X}$ may depend on the axial and circumferential locations of the corrosion defect on the pipeline. For example, defects at a certain location on the pipeline may on average grow faster than the defects at other locations.

Consider the series system representing the wall penetration first. At a given time t, the FORM can be used to evaluate $\text{Prob}[g_i^s(t) \le 0]$ with the corresponding reliability index denoted by $\beta_i^s(t)$. It is noted that because $g_i^s(t)$ monotonically decreases over time as corrosion defects cannot self-heal, $\beta_i^s(t)$ corresponds to the cumulative probability of the ith defect penetrating the pipe wall within the time interval $[0, t]$ (Andrieu-Renaud, Sudret, & Lemaire, 2004). Define $\boldsymbol{\beta}^s(t) = [\beta_1^s(t), \beta_2^s(t), \ldots, \beta_n^s(t)]^{\mathrm{T}}$, and let $\boldsymbol{R}^s(t)$ denote the correlation matrix of the linearised safety margins associated with $g_1^s(t), g_2^s(t), \ldots, g_n^s(t)$ in the standard normal space. The cumulative probability of any of the n defects penetrating the pipe wall within $[0, t]$, $P^s(t)$, then equals $1 - \Phi_n(\boldsymbol{\beta}^s(t), \boldsymbol{R}^s(t))$.

The reliability index, $\beta^{se}(t)$, corresponding to $P^s(t)$ equals $-\Phi^{-1}(P^s(t))$, where $\Phi^{-1}(\bullet)$ is the inverse of $\Phi(\bullet)$. Following Gollwitzer, & Rackwitz (1983) as well as Estes, & Frangopol (1998), we construct a linearised equivalent limit state function at time t, $G^{se}(t)$, in the standard normal space whose reliability index equals $\beta^{se}(t)$. It follows that:

$$G^{se}(t) = \beta^{se}(t) - (\boldsymbol{\alpha}^{se}(t))^{\mathrm{T}}\boldsymbol{u} \tag{7}$$

where $\boldsymbol{u}$ denotes values of the m-dimensional vector of the standard normal variates transformed from $\boldsymbol{X}$, and $\boldsymbol{\alpha}^{se}(t)$ is the equivalent unit normal vector associated with the linearised equivalent limit state function at time t.

Given that the unit normal vector represents the sensitivity of the reliability index with respect to the random variables involved (see Appendix A), $\boldsymbol{\alpha}^{se}(t)$ can be evaluated as (Gollwitzer, & Rackwitz, 1983):

$$\alpha_k^{se}(t) = \frac{\frac{\partial \beta^{se}(t)}{\partial u_k}}{\sqrt{\sum_{k=1}^{m}\left(\frac{\partial \beta^{se}(t)}{\partial u_k}\right)^2}}, \quad (k = 1, 2, \ldots, m) \tag{8}$$

where $\alpha_k^{se}(t)$ is the kth component of $\boldsymbol{\alpha}^{se}(t)$. In this study, $\frac{\partial \beta^{se}(t)}{\partial u_k}$ is computed by utilising the chain rule as follows:

$$\frac{\partial \beta^{se}(t)}{\partial u_k} = \sum_{i=1}^{n} \frac{\partial \beta^{se}(t)}{\partial \beta_i^s(t)} \frac{\partial \beta_i^s(t)}{\partial u_k} \tag{9}$$

In Equation (9), $\frac{\partial \beta_i^s(t)}{\partial u_k}$ is already available from the FORM analysis carried out for the individual limit state function $g_i^s(t)$; therefore, only $\frac{\partial \beta^{se}(t)}{\partial \beta_i^s(t)}$ needs to be evaluated. This can be achieved through the finite difference method. The use of Equation (9) to evaluate the equivalent unit normal vector is more efficient and numerically stable than the approach employed by Gollwitzer, & Rackwitz (1983), which involves directly calculating $\frac{\partial \beta^{se}(t)}{\partial u_k}$ by perturbing the value of u_k at the design point associated with the individual limit state function.

As to the series system for the plastic collapse, FORM can be used to evaluate Prob$[g_i^c(t) \leq 0]$ with the corresponding reliability index denoted by $\beta_i^c(t)$. It is noted that $g_i^c(t)$ is a monotonically decreasing function of time because $p_{ci}(t)$ monotonically decreases over time and because the pipe internal pressure is assumed to be time-independent in this study. Therefore, $\beta_i^c(t)$ represents the cumulative probability of plastic collapse at the ith defect within $[0, t]$. The procedure for constructing $G^{se}(t)$ is equally applicable to construct a linearised equivalent limit state function, $G^{ce}(t)$, for the series system representing the plastic collapse, with the corresponding reliability index $\beta^{ce}(t)$ and equivalent unit normal vector $\boldsymbol{\alpha}^{ce}(t)$, where $\beta^{ce}(t)$ corresponds to the cumulative probability of plastic collapse at any of the n defects within $[0, t]$. With the equivalent limit state functions for the wall penetration and plastic collapse established, the n active defects on the pipeline are now represented by a single equivalent active defect, which greatly simplifies formulations for $P_l(t)$ and $P_b(t)$ as described in the next section.

3.3. Formulations for system failure probabilities of corroding pipelines

As implied by Equation (5), the evaluation of $P_l(t)$ and $P_b(t)$ is a problem of computing the probability of first excursion into the failure region associated with either leak or burst within $[0, t]$. It follows that $P_l(t)$ and $P_b(t)$ must be evaluated incrementally as follows:

$$P_l(\tau + \Delta t) = P_l(\tau) + \Delta P_l(\tau, \Delta t) \tag{10a}$$

$$P_b(\tau + \Delta t) = P_b(\tau) + \Delta P_b(\tau, \Delta t) \tag{10b}$$

where $\Delta P_l(\tau, \Delta t)$ and $\Delta P_b(\tau, \Delta t)$ $(0 \leq \tau < t)$ are incremental probabilities of leak and burst, respectively, within a short time interval between τ and $\tau + \Delta t$. The value of Δt in the range of 0.5 to one year is considered a reasonable choice for the reliability analysis of corroding pipelines, considering that the growth of corrosion on pipelines is typically a slow process.

The geometric descriptions of $\Delta P_l(\tau, \Delta t)$ and $\Delta P_b(\tau, \Delta t)$ in terms of the equivalent limit state functions $G^{se}(\tau)$ and $G^{ce}(t)$ are shown in Figure 2(a) and (b), respectively. Four hyperplanes representing $G^{ce}(\tau + \Delta t) = G^{se}(\tau + \Delta t) = G^{ce}(\tau) = G^{se}(\tau) = 0$ respectively are shown in Figure 2. The incremental probabilities of leak and burst as time increases from τ to $\tau + \Delta t$ are depicted as the two shaded areas, in Figure 2(a) and (b), respectively. The grey arrows in Figure 2 point to the design points associated with limit state functions relevant to the calculations of $\Delta P_l(\tau, \Delta t)$ and $\Delta P_b(\tau, \Delta t)$. It follows from Figure 2 that $\Delta P_l(\tau, \Delta t)$ and $\Delta P_b(\tau, \Delta t)$ are given by:

$$\Delta P_l(\tau, \Delta t) = \Phi_3\left(\left[\beta^{se}(\tau), -\beta^{se}(\tau + \Delta t), \beta^{ce}(\tau)\right]^{\mathrm{T}}, \boldsymbol{R}^{sc}(\tau, \Delta t)\right) \tag{11a}$$

$$\Delta P_b(\tau, \Delta t) = \Phi_3\left(\left[\beta^{ce}(\tau), -\beta^{ce}(\tau + \Delta t), \beta^{se}(\tau)\right]^{\mathrm{T}}, \boldsymbol{R}^{cs}(\tau, \Delta t)\right) \tag{11b}$$

where $\boldsymbol{R}^{sc}(\tau, \Delta t)$ is the 3×3 matrix of correlation coefficients of the three linearised equivalent limit state functions $G^{se}(\tau + \Delta t)$, $G^{se}(\tau)$ and $G^{ce}(\tau)$, and $\boldsymbol{R}^{cs}(\tau, \Delta t)$ is the 3×3 matrix of correlation coefficients of $G^{ce}(\tau + \Delta t)$, $G^{ce}(\tau)$ and $G^{se}(\tau)$. The correlation coefficient between $G^{se}(\tau + \Delta t)$ and $G^{se}(\tau)$ equals $(\boldsymbol{\alpha}^{se}(\tau + \Delta t))^{\mathrm{T}}\boldsymbol{\alpha}^{se}(\tau)$; the correlation coefficient between $G^{se}(\tau + \Delta t)$ and $G^{ce}(\tau)$ equals $(\boldsymbol{\alpha}^{se}(\tau + \Delta t))^{\mathrm{T}}\boldsymbol{\alpha}^{ce}(\tau)$, and the other correlation coefficients can be evaluated in a similar fashion.

The area ABCD indicated in Figure 2 corresponds to the probability of the occurrence of both leak and burst within $[\tau, \tau + \Delta t]$. Because it is not feasible for the proposed methodology to determine which failure mode will occur first within this time interval, the area ABCD is included in both $\Delta P_l(\tau, \Delta t)$ and $\Delta P_b(\tau, \Delta t)$. For reasonably small values of Δt, the error introduced by this approximation is considered insignificant. Note that the growth

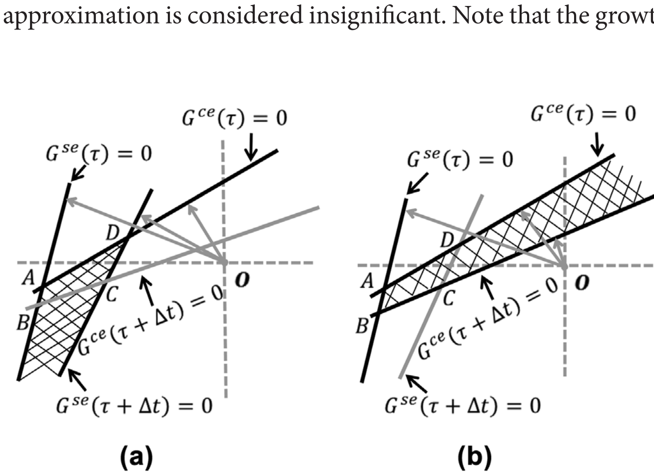

Figure 2. Geometric descriptions of $\Delta P_l(\tau, \Delta t)$ and $\Delta P_b(\tau, \Delta t)$. (a) $\Delta P_l(\tau, \Delta t)$, (b) $\Delta P_b(\tau, \Delta t)$.

of corrosion defects on pipelines is generally a gradual process; therefore, it can be assumed that the hyperplanes corresponding to $G^{se}(\tau) = G^{se}(\tau + \Delta t) = 0$ are parallel to each other and that the hyperplanes corresponding to $G^{ce}(\tau) = G^{ce}(\tau + \Delta t) = 0$ are parallel to each other. In other words, $G^{se}(\tau)$ and $G^{se}(\tau + \Delta t)$ are assumed to be fully correlated, and $G^{ce}(\tau)$ and $G^{ce}(\tau + \Delta t)$ are assumed to be fully correlated.

Based on these assumptions, Equations (11a) and (11b) can be slightly simplified as:

$$\Delta P_l(\tau,\ \Delta t) = \int_{-\infty}^{\beta^{ce}(\tau)} \int_{\beta^{se}(\tau+\Delta t)}^{\beta^{se}(\tau)} \phi_2\left(\theta_1, \theta_2, r^{sc}(\tau)\right) \mathrm{d}\theta_1 \mathrm{d}\theta_2 \quad (12a)$$

$$\Delta P_b(\tau,\ \Delta t) = \int_{-\infty}^{\beta^{se}(\tau)} \int_{\beta^{ce}(\tau+\Delta t)}^{\beta^{ce}(\tau)} \phi_2\left(\theta_1, \theta_2, r^{sc}(\tau)\right) \mathrm{d}\theta_1 \mathrm{d}\theta_2 \quad (12b)$$

where $\phi_2(\bullet, \bullet, \bullet)$ is the probability density function of the bivariate normal distribution, and $r^{sc}(\tau) = (\boldsymbol{\alpha}^{se}(\tau))^{\mathrm{T}}\boldsymbol{\alpha}^{ce}(\tau)$ is the correlation coefficient between $G^{se}(\tau)$ and $G^{ce}(\tau)$. Given the formulations for $\Delta P_l(\tau, \Delta t)$ and $\Delta P_b(\tau, \Delta t)$, $P_l(t)$ and $P_b(t)$ can be evaluated recursively from Equations (10a) and (10b) starting from $P_l(0)$ and $P_b(0)$, which can be evaluated as $\mathrm{Prob}[G^{se}(0) \le 0]$ and $\mathrm{Prob}[G^{ce}(0) \le 0]$, respectively.

4. Numerical examples

4.1. General information

Three examples, which are representative of small-, medium- and large-diameter pipeline segments respectively, are used to illustrate the application and accuracy of the above-described methodology for evaluating the system reliability of corroding pipelines. Table 1 summarises the basic attributes of these examples, which include their nominal outside diameters (D_n), nominal wall thicknesses (wt_n), specified minimum yield strengths (SMYS) and maximum operating pressures (MOP). For illustrative purpose, it is assumed that ten active corrosion defects have been detected and sized by a recently run ILI on each of the three pipeline segments although the methodology can easily cope with more defects.

The initial lengths (l_0) of all ten defects reported by the ILI tool are assumed to equal 50 mm; the ILI-reported initial depths (d_0) of five defects equal $0.25wt_n$, and the initial depths of the other five defects equal $0.3wt_n$. The burst pressure capacity of the segment at a given defect is evaluated using the B31G Modified model as given by Equations (3) and (4). The reduction factor φ in Equation (1) is set to be 0.8.

For simplicity, the following simple linear growth model is adopted to characterise the growth of the defect length over time:

$$l(t) = l_0 + g_l t \quad (14)$$

where g_l is the length growth rate, and t is the forecasting time. In addition, three different defect depth growth models that are widely adopted in the literature are employed, namely the linear, nonlinear and gamma process-based models (Zhou, 2010; Al-Amin & Zhou, 2014; Zhang, & Zhou, 2014; Ellingwood, & Mori, 1997; Valor, Caleyo, Hallen, & Velázquez, 2013). Details of these models are described in the following sections. In practice, the growth of corrosion defects is often quantified through the so-called defect matching procedure, i.e. comparing sizes of the same defect reported in successive ILIs. Extensive studies (Achterbosch, & Grzelak, 2006; Al-Amin, Zhou, Zhang, Kariyawasam, & Wang, 2014; Zhang, Zhou, Al-Amin, Kariyawasam, & Wang, 2014) have been reported in the literature for quantifying various growth models based on the defect sizes reported by multiple ILIs, while taking into account the measurement errors associated with the ILI results.

The probabilistic characteristics of all parameters except for the defect depth growth are summarised in Table 2. Note that the uncertainties in d_0 and l_0 are intended to reflect the measurement errors associated with the ILI tools, which can be quantified from typical accuracy specifications of the tool such as the measured depth (length) being within $\pm 5\% wt_n$ (10 mm) of the actual depth (length). Note further that the pipe internal pressure is in general bounded (Canadian Standards Association (CSA), 2015); however, for simplicity but without affecting the objective of the numerical examples, the internal pressure is assumed to be characterised by an unbounded distribution (Gumbel distribution) based on the findings of the well-known SUPERB project (Jiao, Sotberg, & Igland, 1995).

Moreover, Table 2 presents the assumed correlation coefficient (ρ_1) between random variables representing the same physical parameter at different defects. Random variables associated with the same defect may also be correlated (e.g. the growths of the defect depth and length); such correlations can be easily accounted for in the analysis but are ignored for the sake of simplicity. The spatial correlation between the growths of different defects can be quantified based on the results obtained from the defect matching practice; however, the measurement errors of the ILI tools as well as the potential spatial correlation associated with the measurement errors make this a challenging task. In the present study, parametric analyses with respect to the spatial correlation between the defect growths are carried out.

The correlation coefficient between non-normally distributed random variables can be modified using the empirical equations

Table 1. Basic attributes of three pipeline examples.

Example	D_n (mm)	wt_n (mm)	SMYS (MPa)	MOP (MPa)
1	324	4.32	359	5
2	610	7.16	414	6
3	914	13.15	483	10

Table 2. Probabilistic characteristics of parameters excluding the defect depth growth.

Parameter	Distribution	Mean	Coefficient of variation (COV) (%)	Corr. coef. at different defects (ρ_1)
D	Deterministic	D_n	–	–
wt	Normal	wt_n	1.5	0.2 or 0.8
σ_y	Normal	1.1SMYS	3.5	
p	Gumbel	1.05MOP	3.0	
l_0	Normal	50 (mm)	15	
d_0	Normal	$0.25/0.3wt_n$	15	
g_l	Weibull	3.0 (mm/year)	15	
ξ	Gumbel	1.297	25.8	

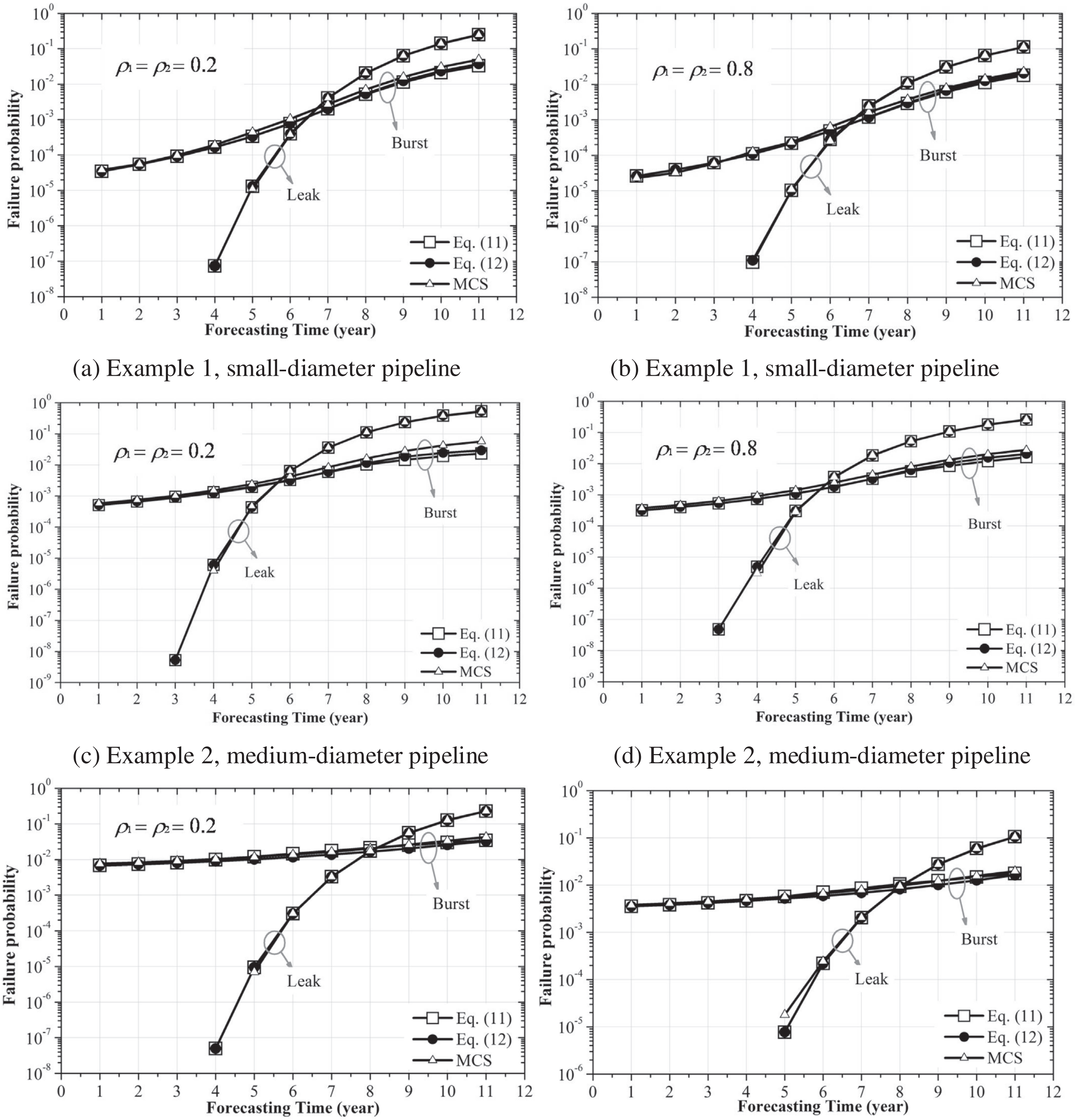

(a) Example 1, small-diameter pipeline
(b) Example 1, small-diameter pipeline
(c) Example 2, medium-diameter pipeline
(d) Example 2, medium-diameter pipeline
(e) Example 3, large-diameter pipeline
(f) Example 3, large-diameter pipeline

Figure 3. Probabilities of burst and leak for examples 1, 2 and 3 based on the linear growth model for defect depth.

provided in (Der Kiureghian, & Liu, 1986) to estimate the corresponding correlation coefficient in the normal space. For simplicity and without affecting the purpose of the examples, the unmodified correlation coefficients are employed in the analysis. To verify the failure probabilities evaluated by using the proposed methodology, the simple MCS with 10^6 simulation trials is performed to evaluate the benchmark failure probability of each example.

4.2. Linear growth model for defect depth

The growth of the defect depth is characterised by:

$$d(t) = d_0 + g_d t \tag{15}$$

where g_d is the constant (but uncertain) depth growth rate. A Weibull distribution with a COV of 50% is assigned to g_d, with the corresponding mean value assumed to equal 0.1, 0.2 and

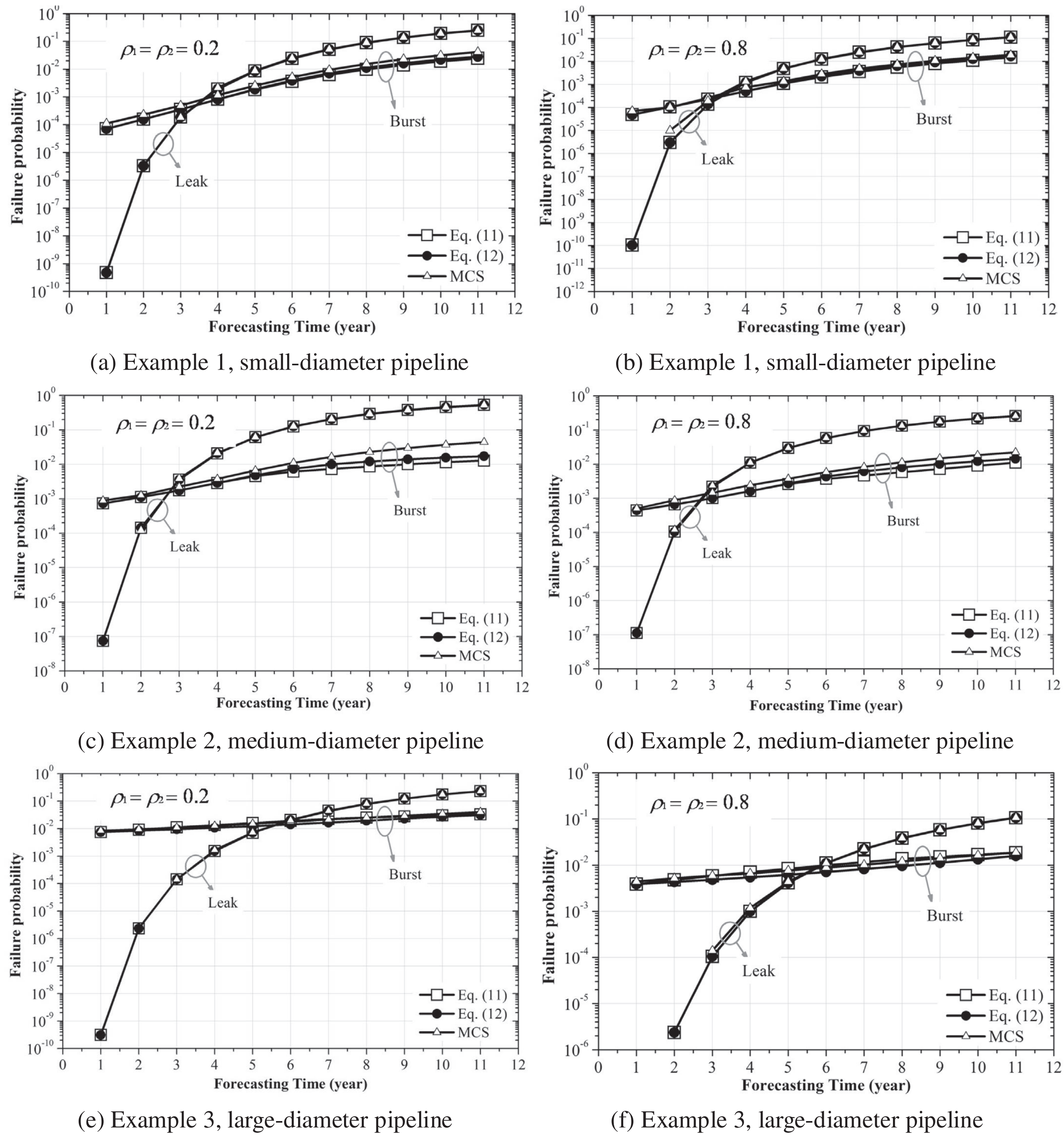

Figure 4. Probabilities of burst and leak for examples 1, 2 and 3 based on the nonlinear growth model for defect depth.

0.3 mm/year for examples 1, 2 and 3, respectively. The growth rates at different defects on a given pipeline segment are assumed to be equicorrelated, with the correlation coefficient ρ_2 equal to 0.2 or 0.8.

The results of the time-dependent system reliability analyses are shown in Figure 3. Note that the probabilities of burst and leak obtained by using Equation (12) (i.e. based on the parallel hyperplane assumption) are shown along with those obtained by using Equation (11) (i.e. without the parallel hyperplane assumption). Moreover, the probabilities of burst and leak obtained from the simple MCS are shown in Figure 3 as the benchmark results. Because the number of simulation trials included in MCS equals 10^6, the lowest failure probability corresponding to MCS shown in Figure 3 is 10^{-6}.

Figure 3 indicates that the failure probabilities corresponding to Equations (11) and (12) are practically identical, therefore validating the assumption that the hyperplane represented by $G^{se}(\tau) = 0$ ($G^{ce}(\tau) = 0$) is parallel to that represented by $G^{se}(\tau + \Delta t) = 0$ ($G^{ce}(\tau + \Delta t) = 0$). The probabilities of leak evaluated by using the proposed methodology are essentially the

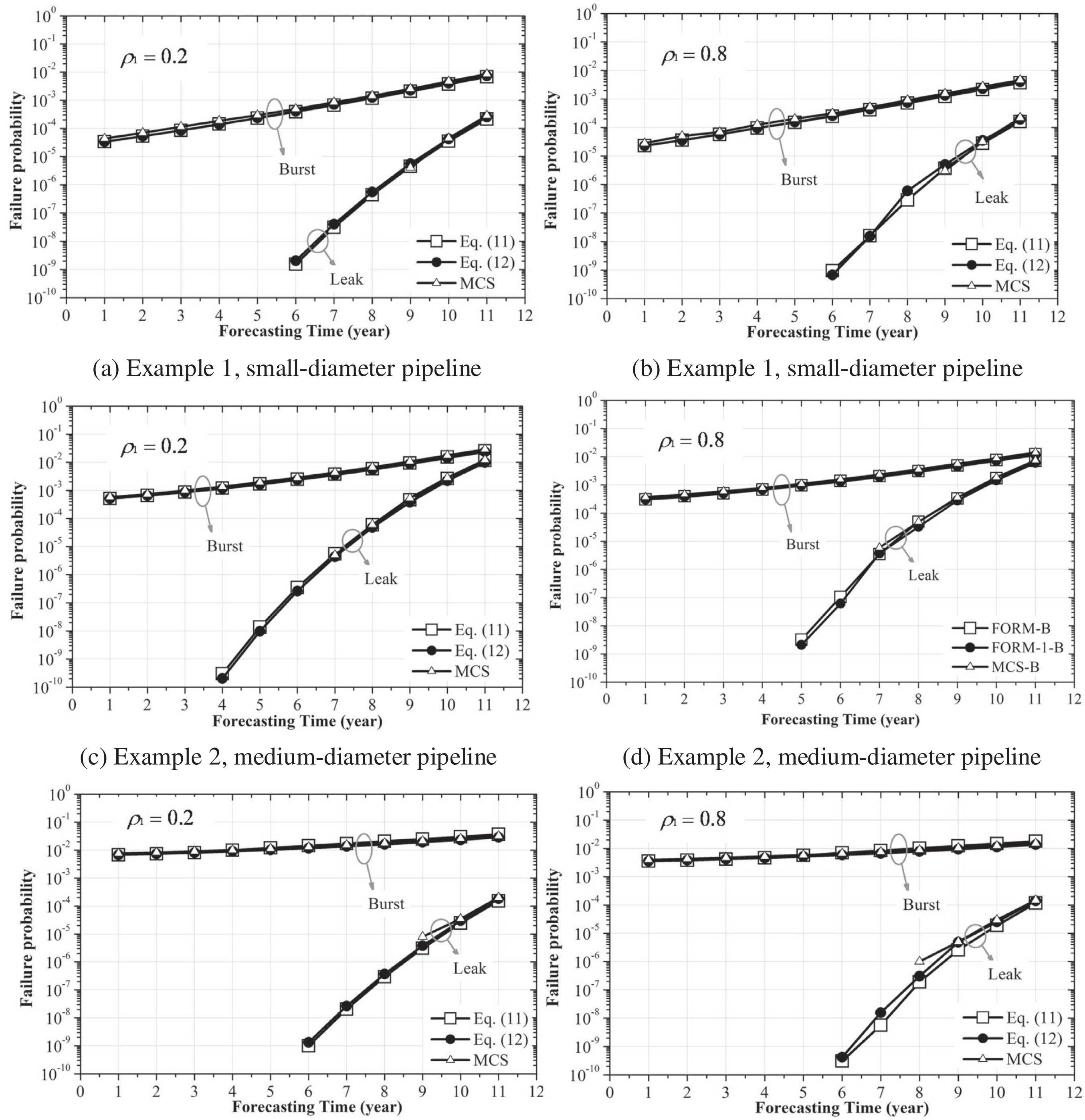

(a) Example 1, small-diameter pipeline
(b) Example 1, small-diameter pipeline
(c) Example 2, medium-diameter pipeline
(d) Example 2, medium-diameter pipeline
(e) Example 3, large-diameter pipeline
(f) Example 3, large-diameter pipeline

Figure 5. Probabilities of burst and leak for examples 1, 2 and 3 based on the homogeneous gamma process-based growth model for defect depth.

same as the corresponding failure probabilities obtained from MCS for all three examples and the two values (i.e. 0.2 and 0.8) of ρ_1 and ρ_2 considered. The probabilities of burst evaluated by using the proposed methodology also in general agree very well with the corresponding MCS results. The proposed methodology tends to slightly underestimate the probabilities of burst for the small- and medium-diameter pipelines as shown in Figures 3(a) through 3(d), but slightly overestimate the probabilities of burst for the large-diameter pipeline as shown in Figures 3(e) and (f).

4.3. Nonlinear growth model for defect depth

A nonlinear power-law growth model (Ellingwood, & Mori, 1997; Valor et al., 2013) is employed to characterise $d(t)$ as follows:

$$d(t) = d_0 + kt^{\gamma} \tag{16}$$

where k and γ are the parameters of the power-law growth model. In general, the variability of k is large, but the variability of γ is small (Ellingwood, & Mori, 1997). Therefore, γ is assumed in this study to be a deterministic quantity that equals 0.5, whereas k is characterised by a Weibull variate with a COV of 50%. The mean value of k is assumed to equal 0.332, 0.663 and 0.995 mm/year$^{0.5}$ for examples 1, 2 and 3, respectively. Furthermore, the Weibull variates representing k for different defects are assumed to be equicorrelated, with the correlation coefficient ρ_2 equal to 0.2 or 0.8.

The probabilities of burst and leak obtained from the proposed methodology and simple MCS for the nonlinear growth model of the defect depth are depicted in Figure 4. This figure leads to similar observations as those from Figure 3. First, the validity of the parallel hyperplane assumption is further demonstrated in Figure 4 as the results corresponding to Equations (11) and (12) are the same. Second, the probabilities of leak corresponding to the proposed methodology are in excellent agreement with those from MCS for all three examples. The proposed methodology somewhat underestimates the probabilities of burst for small- and medium-diameter pipelines, especially the latter case as shown in Figures 4(c) and (d), but the difference is considered acceptable. Finally, the proposed methodology slightly overestimates the probabilities of burst for the large-diameter pipeline as shown in Figures 4(e) and (f).

4.4. Gamma process-based growth model for defect depth

The homogeneous gamma process (van Noortwijk, 2009) is employed to characterise the growth of the defect depth as follows:

$$d(t) = d_0 + d_g(t) \tag{17}$$

where $d_g(t)$ denotes the homogeneous gamma process. The probability density function of the gamma-distributed $d_g(t)$, $F(d_g(t)|at, b)$, is given by:

$$F\left(d_g(t)|at, b\right) = b^{at}(d_g)^{at-1}\exp\left(-bd_g\right)/\Gamma(at) \tag{18}$$

where a and b are parameters of the gamma process, and $\Gamma(\bullet)$ is the gamma function. It follows from the properties of the gamma process (van Noortwijk, 2009) that $d_g(\tau + \Delta t) = d_g(\tau) + d_g(\Delta t)$, where $d_g(\Delta t)$ is the gamma-distributed increment of the defect depth within Δt and is independent of $d_g(\tau)$. The correlation coefficient between $d_g(\tau + \Delta t)$ and $d_g(\tau)$, $\rho_g(\tau, \Delta t)$, can be shown to equal $\sqrt{\frac{\tau}{\tau+\Delta t}}$ (see Appendix B for the derivation). If Equation 11(a) and (b) (as opposed to Equation 12(a) and (b)) are used to evaluate $\Delta P_l(\tau, \Delta t)$ and $\Delta P_b(\tau, \Delta t)$ respectively, $\rho_g(\tau, \Delta t)$ needs to be accounted for in the evaluation of $\boldsymbol{R}^{sc}(\tau, \Delta t)$ and $\boldsymbol{R}^{cs}(\tau, \Delta t)$.

Let μ and σ denote, respectively, the mean and standard deviation of the depth increment within one year. The parameters of the gamma process, a and b, are related to μ and σ as $\mu = a/b$ and $\sigma^2 = a/b^2$ (van Noortwijk, 2009). In this study, a is assumed to equal 4, whereas b is assumed to equal 40, 20 and 13.33 (mm/year)$^{-1}$ for examples 1, 2 and 3, respectively. This corresponds to μ (σ) = 0.1 (0.05), 0.2 (0.1) and 0.3 (0.15) mm/year for examples 1, 2 and 3, respectively. For simplicity, the gamma processes $d_g(t)$ at different defects are assumed to be mutually independent.

Figure 5 depicts the failure probabilities obtained from the proposed methodology and MCS for the gamma process-based defect depth growth. The figure indicates that the failure probabilities obtained from the proposed methodology agree very well with those obtained from MCS for all three examples and $\rho_1 = 0.2$ and 0.8. Finally, the results shown in Figures 3–5 demonstrate the applicability of the proposed methodology for both random variable- and stochastic process-based defect growth models and accuracy of the methodology.

5. Conclusions

A FORM-based methodology is proposed in this study to evaluate the time-dependent system reliability of a segment of pressurised steel pipeline containing multiple active corrosion defects. The methodology considers two competing failure modes of the pipe segment, i.e. leak and burst, and takes into account correlations among limit state functions at different defects. At a given time, the FORM is applied to the limit state functions corresponding to the defect penetrating the pipe wall and plastic collapse at individual corrosion defects on the pipe segment. Two linearised equivalent limit state functions, corresponding to the defect penetrating the pipe wall and plastic collapse respectively, are then established in the standard normal space for all the defects on the pipe segment. The unit normal vectors associated with the equivalent limit state functions are computed using the chain rule that incorporates the sensitivity factors obtained from the FORM analysis for each individual defect. Based on the equivalent limit state functions, a procedure is developed to incrementally evaluate the probabilities of leak and burst for the pipe segment over a forecasting time period.

The proposed methodology is applied to three numerical examples that are representative of small-, medium- and large-diameter pipeline segments. Each example is assumed to contain ten active corrosion defects. Furthermore, three widely used models are adopted to characterise the growth of the defect depth, namely the linear, nonlinear and homogeneous gamma process-based growth models. The probabilities of leak and burst of the examples evaluated by using the proposed methodology are compared with those obtained from the simple Monte Carlo simulation. The comparison indicates that the proposed methodology is accurate for different defect growth models and various levels of correlations among limit state functions at different defects.

Acknowledgements

The financial supported provided by the Faculty of Engineering at the University of Western Ontario and Discovery Grant Program (RGPIN-2014-05232) of the Natural Sciences and Engineering Research Council of Canada (NSERC) is gratefully acknowledged. The authors thank the anonymous reviewers for their constructive comments and suggestions that led to marked improvement of the paper.

Disclosure statement

No potential conflict of interest was reported by the authors.

Funding

This work was supported by Natural Sciences and Engineering Research Council of Canada [RGPIN-2014-05232].

References

Achterbosch, G.G.J., & Grzelak, L.A. (2006). Determination of the corrosion rate of a MIC influenced pipeline using four consecutive pig runs. *Proceedings of the International Pipeline Conference (IPC2006), IPC2006-10142, ASME*. Calgary.

Al-Amin, M., & Zhou, W. (2014). Evaluating the system reliability of corroding pipelines based on inspection data. *Structure and Infrastructure Engineering, 10*, 1161–1175.

Al-Amin, M., Zhou, W., Zhang, S., Kariyawasam, S., & Wang, H. (2014). Hierarchical Bayesian corrosion growth model based on in-line inspection data. *Journal of Pressure Vessel Technology, 136*, 041401.

Andrieu-Renaud, C., Sudret, B., & Lemaire, M. (2004). The PHI2 method: A way to compute time-variant reliability. *Reliability Engineering & System Safety, 84*, 75–86.

Caleyo, F., Gonzalez, J.L., & Hallen, J.M. (2002). A study on the reliability assessment methodology for pipelines with active corrosion defects. *International Journal of Pressure Vessels and Piping, 79*, 77–86.

Canadian Standards Association (CSA). (2015). *CSA Z662: Oil and gas pipeline systems*. Mississauga: Canadian Standards Association.

Der Kiureghian, A. (2005). First- and second-order reliability methods. In E. Nikolaidis, D. M. Ghiocel, & S. Singhal (Eds.), *Engineering design reliability handbook* (Chap. 14, pp. 1–14). Boca Raton: CRC Press.

Der Kiureghian, A., & Liu, P.L. (1986). Structural reliability under incomplete probability information. *Journal of Engineering Mechanics, 112*, 85–104.

Ellingwood, B.R., & Mori, Y. (1997). Reliability-based service life assessment of concrete structures in nuclear power plants: Optimum inspection and repair. *Nuclear Engineering and Design, 175*, 247–258.

Estes, A.C., & Frangopol, D.M. (1998). RELSYS: A computer program for structural system reliability. *Structural Engineering and Mechanics, 6*, 901–919.

Genz, A. (1992). Numerical computation of multivariate normal probabilities. *Journal of Computational and Graphical Statistics, 1*, 141–149.

Gollwitzer, S., & Rackwitz, R. (1983). Equivalent components in first-order system reliability. *Reliability Engineering, 5*, 99–115.

Gomes, W.J., & Beck, A.T. (2014). Optimal inspection and design of onshore pipelines under external corrosion process. *Structural Safety, 47*, 48–58. Retrieved October, 2015, from http://www.math.wsu.edu/faculty/genz/software/software.html

Huyse, L., & Brown, K.A. (2012). Why reliability-based approaches need more realistic corrosion growth modeling. *9th International Pipeline Conference (IPC2012), ASME, IPC2012-90319*. Calgary.

Jiao, G., Sotberg, T., & Igland, R.T. (1995). *SUPERB 2M statistical data-basic uncertainty measures for reliability analysis of offshore pipelines* (SUPERB JIP Report No. STF70-F95212). Trondheim: Norwegian Marine Technology Research Institute.

Kariyawasam, S., & Peterson, W. (2010). Effective improvements to reliability based corrosion management. *8th International Pipeline Conference (IPC2010), ASME, IPC2010-31425*. Calgary.

Kiefner, J.F., & Vieth, P.H. (1989). *A modified criterion for evaluating the remaining strength of corroded pipe* (No. PR-3-805). Columbus, OH: Battelle Columbus Div. Retrieved from http://www.osti.gov/scitech/biblio/7181509

Leira, B.J., Næss, A., & Næss, O.E.B. (2016). Reliability analysis of corroding pipelines by enhanced Monte Carlo simulation. *International Journal of Pressure Vessels and Piping, 144*, 11–17.

Low, B.K., & Tang, W.H. (2007). Efficient spreadsheet algorithm for first-order reliability method. *Journal of Engineering Mechanics, 133*, 1378–1387.

Lu, D., Xie, W.C., & Pandey, M.D. (2013). An efficient method for the estimation of parameters of stochastic gamma process from noisy degradation measurements. *Proceedings of the Institution of Mechanical Engineers, Part O: Journal of Risk and Reliability, 227*, 425–433.

Melchers, R.E. (1999). *Structural reliability analysis and prediction.* New York: John Wiley & Sons.

Miran, S.A., Huang, Q., & Castaneda, H. (2016). Time-dependent reliability analysis of corroded buried pipelines considering external defects. *Journal of Infrastructure Systems, 22*, 04016019.

Nessim, M., Zhou, W., Zhou, J., & Rothwell, B. (2009). Target reliability levels for design and assessment of onshore natural gas pipelines. *Journal of Pressure Vessel Technology, 131*(6), 061701.

van Noortwijk, J.M. (2009). A survey of the application of gamma processes in maintenance. *Reliability Engineering & System Safety, 94*(1), 2–21.

Sahraoui, Y., Khelif, R., & Chateauneuf, A. (2013). Maintenance planning under imperfect inspections of corroded pipelines. *International Journal of Pressure Vessels and Piping, 104*, 76–82.

Teixeira, A.P., Soares, C.G., Netto, T.A., & Estefen, S.F. (2008). Reliability of pipelines with corrosion defects. *International Journal of Pressure Vessels and Piping, 85*, 228–237.

Valor, A., Caleyo, F., Hallen, J.M., & Velázquez, J.C. (2013). Reliability assessment of buried pipelines based on different corrosion rate models. *Corrosion Science, 66*, 78–87.

Zhang, S., & Zhou, W. (2014). An efficient methodology for the reliability analysis of corroding pipelines. *Journal of Pressure Vessel Technology, 136*(4), 041701.

Zhang, S., Zhou, W., Al-Amin, M., Kariyawasam, S., & Wang, H. (2014). Time-dependent corrosion growth modeling using multiple in-line inspection data. *Journal of Pressure Vessel Technology, 136*, 041202-1–041202-7.

Zhou, W. (2010). System reliability of corroding pipelines. *International Journal of Pressure Vessels and Piping, 87*, 587–595.

Zhou, W., & Huang, G.X. (2012). Model error assessments of burst capacity models for corroded pipelines. *International Journal of Pressure Vessels and Piping, 99*, 1–8.

Appendix A. Summary of the formulations for the FORM

The failure probability, P_f, of an engineering system can be represented by the following multidimensional integral:

$$P_f = \int_{g(\boldsymbol{x})\leq 0} f_{\boldsymbol{X}}(\boldsymbol{x})\mathrm{d}\boldsymbol{x} \tag{A.1}$$

where $\boldsymbol{x}$ denotes values of a vector of m random variables $\boldsymbol{X} = [X_1, X_2, \ldots, X_m]^{\mathrm{T}}$; $g(\boldsymbol{x})$ is the limit state function with $g(\boldsymbol{x}) > 0$ and $g(\boldsymbol{x}) < 0$ defining the safe and failure domains, respectively; $g(\boldsymbol{x}) = 0$ is known as the limit state surface, and $f_{\boldsymbol{X}}(\boldsymbol{x})$ is the joint probability density function of $\boldsymbol{X}$.

To employ FORM to approximately evaluate P_f, $\boldsymbol{X}$ is first transformed to $\boldsymbol{Z} = [Z_1, Z_2, \ldots, Z_m]^{\mathrm{T}}$, and then $\boldsymbol{Z}$ is transformed to $\boldsymbol{U} = [U_1, U_2, \ldots, U_m]^{\mathrm{T}}$, where Z_i ($i = 1,\ldots, m$) are correlated normal variates with zero means and unity variances, and U_i are independent and standard normal variates. The reliability index β is then obtained by solving the following constrained optimisation problem (Der Kiureghian 2005; Low, & Tang 2007):

$$\beta = \min \sqrt{\boldsymbol{z}^{\mathrm{T}}\boldsymbol{R}_{zz}^{-1}\boldsymbol{z}}, \quad \text{subject to } g_Z(\boldsymbol{z}) = 0 \tag{A.2}$$

or:

$$\beta = \min \sqrt{\boldsymbol{u}^{T}\boldsymbol{u}}, \quad \text{subject to } g_U(\boldsymbol{u}) = 0 \tag{A.3}$$

where $\boldsymbol{z}$ denotes the value of $\boldsymbol{Z}$; $\boldsymbol{u}$ denotes the value of $\boldsymbol{U}$; $\boldsymbol{R}_{ZZ}$ is the correlation matrix of $\boldsymbol{Z}$, $g_Z(\boldsymbol{z}) = g(\boldsymbol{x}(\boldsymbol{z}))$ is the limit state function in terms of $\boldsymbol{z}$; $\boldsymbol{x}(\boldsymbol{z})$ denotes that $\boldsymbol{x}$ is a function of $\boldsymbol{z}$; $g_U(\boldsymbol{u}) = g(\boldsymbol{x}(\boldsymbol{z}(\boldsymbol{u})))$ is the limit state function in terms of $\boldsymbol{u}$, and $\boldsymbol{z}(\boldsymbol{u})$ denotes that $\boldsymbol{z}$ is a function of $\boldsymbol{x}$.
The inverse normal transformation can be used to transform X_i to Z_i ($i = 1, \ldots, m$) (Der Kiureghian 2005), i.e.:

$$z_i = \Phi^{-1}(F_{X_i}(x_i)) \tag{A.4}$$

where $F_{X_i}(x_i)$ denotes CDF of X_i, and $\Phi^{-1}(\bullet)$ is the inverse of the standard normal CDF. Let $\boldsymbol{R}_{XX}$ denote the correlation matrix of $\boldsymbol{X}$. The components of $\boldsymbol{R}_{ZZ}$ can be obtained from the corresponding components of $\boldsymbol{R}_{XX}$ using the empirical equations proposed by Der Kiureghian, & Liu (1986) for the Nataf transformation. The transformation from $\boldsymbol{Z}$ to $\boldsymbol{U}$ is carried out as:

$$\boldsymbol{U} = \boldsymbol{L}^{-1}\boldsymbol{Z} \tag{A.5}$$

where $\boldsymbol{L}$ is the lower-triangular matrix obtained from the Cholesky decomposition of $\boldsymbol{R}_{ZZ}$ (Der Kiureghian 2005). Let $\boldsymbol{u}^*$ denote the solution (i.e. design point) to Equation (A.3).

The unit normal vector, $\boldsymbol{\alpha}$, that is normal to $g_U(\boldsymbol{u}) = 0$ at $\boldsymbol{u}^*$ and pointing toward the failure domain is computed from (Der Kiureghian, 2005):

$$\boldsymbol{\alpha} = \boldsymbol{u}^*/\beta \tag{A.6}$$

It follows that $g_U(\boldsymbol{u})$ can be approximated by a linearised limit state function (or safety margin), $G_U(\boldsymbol{u})$, given by:

$$G_U(\boldsymbol{u}) = \beta - \boldsymbol{\alpha}^{\mathrm{T}}\boldsymbol{u} \tag{A.7}$$

The hyperplane $G_U(\boldsymbol{u}) = 0$ then represents the linearised limit state surface. Note that the solution to Equation (A.2), $\boldsymbol{z}^*$, can be straightforwardly transformed to $\boldsymbol{u}^*$ by using Equation (A.5), which then allows the computation of $\boldsymbol{\alpha}$. It follows from Equation (A.7) that:

$$\boldsymbol{\alpha} = \left.\frac{\partial\beta}{\partial\boldsymbol{u}}\right|_{\boldsymbol{u}=\boldsymbol{u}^*} \tag{A.8}$$

Therefore, components of $\boldsymbol{\alpha}$ are measures of the sensitivity of β to values of the corresponding random variables at the design point.

Appendix B. Derivation of the correlation coefficient between $d_g(\tau + \Delta t)$ and $d_g(\tau)$

Let $E[\bullet]$ and $V[\bullet]$ denote the expectation and variance, respectively, of a random variable $\bullet$. The properties of the gamma process imply that $d_g(\tau + \Delta t) = d_g(\tau) + d_g(\Delta t)$. It follows that:

$$\rho_g(\tau, \Delta t) = \frac{E\left[\left(d_g(\tau) + d_g(\Delta t)\right)d_g(\tau)\right] - E\left[d_g(\tau + \Delta t)\right]E\left[d_g(\tau)\right]}{\sqrt{V\left[d_g(\tau + \Delta t)\right]V\left[d_g(\tau)\right]}} \tag{B.1}$$

where $E\left[\left(d_g(\tau)\right)^2\right] = \left(E\left[d_g(\tau)\right]\right)^2 + V\left[d_g(\tau)\right]$.

Because $d_g(t)$ is a homogeneous gamma process with parameters a and b defined in Equation (18), the expectations of $d_g(\tau + \Delta t)$, $d_g(\tau)$ and $d_g(\Delta t)$ are given by:

$$E\left[d_g(\tau + \Delta t)\right] = a(\tau + \Delta t)/b \tag{B.2}$$

$$E\left[d_g(\tau)\right] = a\tau/b \tag{B.3}$$

$$E\left[d_g(\Delta t)\right] = a(\Delta t)/b \tag{B.4}$$

The variances of $d_g(\tau + \Delta t)$ and $d_g(\tau)$ are given by:

$$V\left[d_g(\tau + \Delta t)\right] = a(\tau + \Delta t)/b^2 \tag{B.5}$$

$$V\left[d_g(\tau)\right] = a\tau/b^2 \tag{B.6}$$

Substituting Equation (B.2) through (B.6) into Equation (B.1) and considering that $d_g(\tau)$ and $d_g(\Delta t)$ are independent of each other lead to $\rho_g(\tau, \Delta t) = \sqrt{\frac{\tau}{\tau+\Delta t}}$.